

2015

Solar Energy Resource Assessment Using R.SUN In GRASS GIS And Site Suitability Analysis Using AHP For Groundmounted Solar Photovoltaic (PV) Farm In The Central Luzon Region (Region 3), Philippines

Ben Hur Pintor

University of the Philippines Diliman

Eula Fae Sola

University of the Philippines Diliman

Justine Teves

University of the Philippines Diliman

Loureal Camille Inocencio

University of the Philippines Diliman

Ma. Rosario Concepcion Ang

University of the Philippines Diliman

Follow this and additional works at: <https://scholarworks.umass.edu/foss4g>

 Part of the [Geography Commons](#)

Recommended Citation

Pintor, Ben Hur; Sola, Eula Fae; Teves, Justine; Inocencio, Loureal Camille; and Ang, Ma. Rosario Concepcion (2015) "Solar Energy Resource Assessment Using R.SUN In GRASS GIS And Site Suitability Analysis Using AHP For Groundmounted Solar Photovoltaic (PV) Farm In The Central Luzon Region (Region 3), Philippines," *Free and Open Source Software for Geospatial (FOSS4G) Conference Proceedings*: Vol. 15 , Article 3.

DOI: <https://doi.org/10.7275/R5N58JKF>

Available at: <https://scholarworks.umass.edu/foss4g/vol15/iss1/3>

SOLAR ENERGY RESOURCE ASSESSMENT USING R.SUN IN GRASS GIS AND SITE SUITABILITY ANALYSIS USING AHP FOR GROUND-MOUNTED SOLAR PHOTOVOLTAIC (PV) FARMS IN THE CENTRAL LUZON REGION (REGION 3), PHILIPPINES

Ben Hur Pintor¹, Eula Fae Sola¹, Justine Teves¹, Loureal Camille Inocencio¹, and Ma. Rosario Concepcion Ang¹

¹Phil-LiDAR 2: Project 5 – REMap, University of the Philippines Diliman
Quezon City 1101, Philippines
Email: bhs.pintor@gmail.com

ABSTRACT

In the study, the solar energy resource in the Central Luzon Region (Region 3), Philippines was determined using r.sun – a topography-based solar radiation model implemented in GRASS GIS – and suitable sites for the installation of ground-mounted solar photovoltaic (PV) farms were identified using the Analytic Hierarchy Process (AHP) to determine the weights of different physical, environmental, socio-economic, risk, and constraint criteria.

For the resource assessment, the inputs to r.sun used in the study consisted of freely available data that include: an SRTM (90m resolution) Digital Elevation Model (DEM) and monthly average Linke turbidity coefficients available from the SoDA (Solar Radiation Database) webservice (www.soda-is.com). Daily solar radiation data from eight (8) measuring stations throughout the region were gathered. Readings from six (6) stations were used to interpolate monthly clear-sky index rasters while the readings from the remaining two (2) stations were used to validate the modelled monthly average Global Horizontal Irradiation (GHI) computed by r.sun.

For the site suitability analysis, different criteria rasters were created and combined using weighted overlay to generate a suitability map for ground-mounted solar PV farms in the region.

From the results, the monthly average GHI in the region computed by r.sun ranged from 3706.8 Wh/m²-day in December to 6021.0 Wh/m²-day in May with an annual average GHI of 4727.12 Wh/m²-day indicating a good amount of resource potential. High GHI values were observed for the summer months of March to May (Mean: 5640.26 Wh/m²-day) while the cold and rainy season ranging from July to December showed relatively lower values (Mean: 4298.98 Wh/m²-day). The Mean Absolute Error (MAE) and Mean Absolute Percentage Error (MAPE) between the measured and modelled GHI were 352.88 Wh/m²-day and 8.53%, respectively, with the lowest error in March (73.94 Wh/m²-day, 1.44%) and the highest in August (844.01 Wh/m²-day, 21.65%). In fact, the model performed well for the months of January to June (MAE: 192.18 Wh/m²-day, MAPE: 3.83%) and slightly poorer for July to December (MAE: 512.824 Wh/m²-day, MAPE: 13.22%).

For further study, other data sources and inputs can be looked into to improve the accuracy of the resource assessment and site suitability analysis. Aside from this, the use of more solar radiation recording stations for validation is preferred in order to better validate the results of r.sun and its applicability for solar energy resource assessment in the Philippines.

1. INTRODUCTION

1.1 Background and Study Area

Solar energy is quickly gaining popularity as a choice for small-scale and large-scale power generation in the Philippines through the use of solar photovoltaic (PV) panels and solar PV farms which have been found to be robust, scalable, and largely sustainable (Nguyen and Pearce, 2010). As of the end of April 2015, the country's Department of Energy

(DOE) has awarded a total of 82 Grid-Use Solar Energy Projects under the Renewable Energy (RE) Law with a total potential capacity of 1,749.53 MW with 42 more projects pending approval for an additional potential capacity of 1,520.14 MW. Among the different sources of renewable energy in the country, the values for solar in terms of the number of projects and total potential capacity rank 2nd only to hydro power (DOE, Awarded Solar Projects as of 30 April 2015). However, solar energy is still very much under-appreciated and under-utilized, accounting for only 0.02% share of the total gross power generation of the country in 2014 (DOE, 2014 Philippine Power Statistics). In order to effectively utilize solar energy as a source of power, especially for large-scale applications such as solar PV farms, the reliable estimation of the solar radiation received in an area is necessary because even though the solar radiation hitting the top of the earth's atmosphere is relatively constant, the radiation that reaches the Earth's surface varies due to factors such as the location, the time, the effects of terrain, and the attenuation caused by the atmosphere. Furthermore, in order to identify locations suitable for setting-up large-scale solar PV farms, several other factors aside from the available solar radiation come into play and need to be considered. The accurate identification of these factors and how they affect the suitability of a location for solar PV farms is important because solar energy projects involve different stakeholders such as the government, the environment, the developers, and the consumers. Finding a site that meets the criteria set forth by the different stakeholders is as important as finding one with high resource potential.

In this study, the solar energy resource in the Central Luzon Region (Region 3), Philippines is assessed using the r.sun model implemented in GRASS (Geographic Resources Analysis and Support System) GIS. Specifically, the monthly average and annual average Global Horizontal Irradiation (GHI) received by the region are computed. In addition to calculating the solar energy resource in the region, site-suitability analysis is performed to find suitable locations for setting-up ground-mounted solar PV farms. Different physical, environmental, socio-economic, risk, and constraint criteria are first identified from related literature as well as interviews with stakeholders and experts. The relative weights of these criteria in terms of how much they affect the suitability of a site for building solar PV farms are determined using the Analytic Hierarchy Process (AHP). Criteria values are standardized and aggregated using Weighted Linear Combination or Weighted Overlay.

The study area is the Central Luzon Region (Figure 1) located between 14° 21' 50" and 16° 31' 48" latitude and 119° 47' 06" and 122° 16' 23" longitude, situated near the heart of the Luzon Island of the Philippine Archipelago. It has seven (7) provinces – Aurora, Bataan, Bulacan, Nueva Ecija, Pampanga, Tarlac, and Zambales – covering a total land area of 18,230.80 km² composed of mountains, extinct and active volcanoes, as well as vast flat farmlands (EMB and ICETT, Green Framework for Innovative Strategy (GFIS) for Sustainable Consumption and Production, 2008). As of April 2015, there are twelve (12) awarded solar projects in the region under the RE Law. One of these projects have already began commercial operation with an installed capacity of 10MW. The remaining eleven have an additional potential capacity of 407 MW. The total potential capacity in the region once all the solar projects are in operation (417 MW) accounts for more than 40% of the expected 985.91 MW capacity of solar projects in the entire Luzon Island (DOE, Awarded Solar Projects as of April 30, 2015).

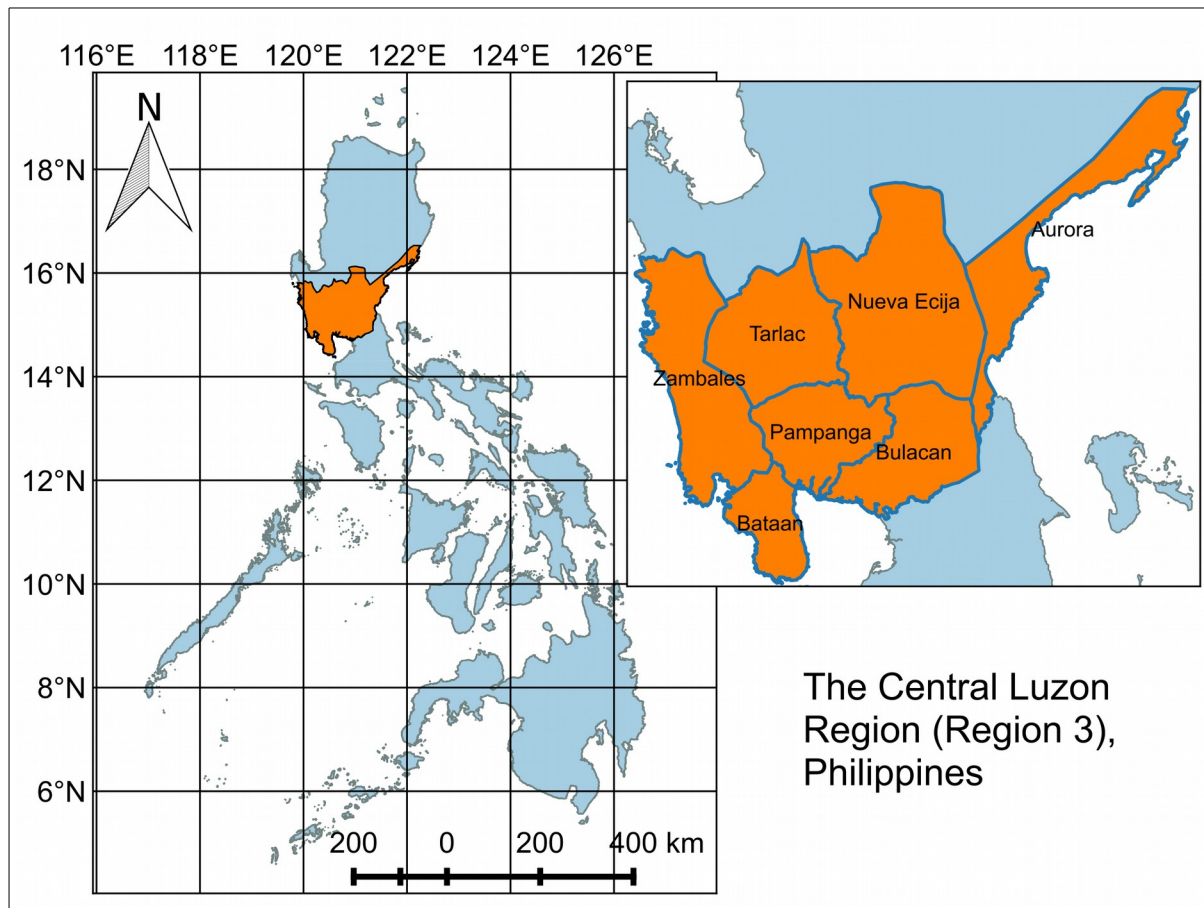


Figure 1. The study area

1.1 Solar Radiation Modelling and r_{sun}

The solar radiation hitting the top of the earth's atmosphere is relatively constant with an accepted value of 1367 W/m^2 but the radiation that reaches the earth's surface varies depending on spatial and temporal factors. There are three groups of factors that determine the interaction of solar radiation with the earth's atmosphere surface (Hofierka and Suri, 2002).

1. the earth's geometry, revolution, and rotation (declination, latitude, solar position)
2. terrain (elevation, surface inclination and orientation, shadowing)
3. atmospheric effects (scattering, absorption) by:
 1. gases (air molecules, ozone, etc.),
 2. solid and liquid particles (aerosols including non-condensed water), and
 3. clouds (condensed water)

The first group determines the available extraterrestrial radiation and can be precisely calculated. The second group considers the effects of topography and can also be modelled with high precision. For the third group, the elevation above sea level determines the attenuation due to the atmosphere's thickness. The attenuation caused by gas particles is given by the relative optical mass and optical thickness – both of which can be calculated at a good level of precision. The Linke turbidity coefficient can be used to describe the effects of solid and liquid particles but due to the dynamic nature of this coefficient, it cannot be modelled at a high level of accuracy. Lastly, the effect of clouds, which are the greatest attenuants, is very difficult to model. As such, simple empirical techniques are often used to estimate the attenuation caused by clouds.

Most solar radiation models compute for solar radiation under clear (cloudless) skies. This is done by disregarding the effects of clouds altogether. However, in reality, actual days with clear skies are hard to come by. In fact, a good assessment of solar energy resource should always account for the effects of clouds. To do this, the clear-sky index (K_c) is often used. The clear-sky index is a value that relates the modelled clear-sky radiation with the actual real-sky radiation measured on the ground (Hofierka and Suri, 2002). There are three ways to estimate K_c (Nguyen and Pearce, 2010):

1. The ratio between the measured and modelled solar radiation.

$$K_c = \frac{\text{radiation}_{\text{measured}}}{\text{radiation}_{\text{modeled}}} \quad (1)$$

2. An empirical formula relating cloudiness (C measured in Oktas) to K_c .

$$K_c = 1 - 0.75 \left(\frac{C}{8} \right) \quad (2)$$

3. Derivation from cloud index values of satellite images.

The first method is the simplest and most commonly used. Using this method, it is necessary to have points where the values for the measured and modelled solar radiation are known. It is important to note that the K_c for the beam and diffused solar radiation is not equal to the K_c for global solar radiation because the ratio of diffuse to global radiation changes relative to cloudiness and are thus computed separately.

$$K_{c_{\text{global}}} = \frac{\text{global}_{\text{measured}}}{\text{global}_{\text{modeled}}} \quad (3)$$

$$K_{c_{\text{beam}}} = \frac{\text{beam}_{\text{measured}}}{\text{beam}_{\text{modeled}}} \quad (4)$$

$$K_{c_{\text{diffuse}}} = \frac{\text{diffuse}_{\text{measured}}}{\text{diffuse}_{\text{modeled}}} \quad (5)$$

The product of the clear-sky radiation and the clear-sky index is the real-sky radiation.

$$\text{global}_{\text{real}} = K_{c_{\text{global}}} \times \text{global}_{\text{modeled}} \quad (6)$$

$$\text{beam}_{\text{real}} = K_{c_{\text{beam}}} \times \text{beam}_{\text{modeled}} \quad (7)$$

$$\text{diffuse}_{\text{real}} = K_{c_{\text{diffuse}}} \times \text{diffuse}_{\text{modeled}} \quad (8)$$

The `r.sun` module implemented in GRASS GIS is a topography-based solar radiation model based on the European Solar Radiation Atlas (ESRA) model. It runs in two modes. Mode 1 computes for the solar incidence angle and solar irradiance (W/m^2) at a specific time of day while Mode 2 computes for the insolation time and solar irradiation ($\text{Wh}/\text{m}^2\text{-day}$) for a specific day of the year. Both modes compute for the global solar radiation and its three components – beam, diffused, and ground-reflected solar radiation – based on time, location, as well as surface and atmospheric conditions. Its inputs are an elevation raster and the day of the year. Location values are provided by latitude and longitude rasters or internal computations. Shadowing is computed internally or through the use of horizon raster maps outputted by the `r.horizon` module. Other parameters such as the slope, aspect, Linke turbidity coefficients, and albedo can be provided as constants, rasters, or have default values. The outputs are raster maps for beam, diffused, ground-reflected, and global solar irradiance or irradiation. Raster maps for the solar incidence angle for Mode 1 and insolation time for Mode 2 are also outputted (GRASS Development Team, 2015).

As a solar radiation model, the strengths of r.sun are (Hofierka and Cebecauer, 2008):

1. it accounts for the effects of topography on incoming solar radiation;
2. it can use rasters as inputs making it highly scalable;
3. the source-code is editable (open-source); and
4. its implementation in GRASS GIS enables it to integrate spatial and non-spatial data and provides for a wide variety of pre-processing, processing, and analysis tools.

1.3 The Analytic Hierarchy Process (AHP)

The Analytic Hierarchy Process (AHP) is a multi-criteria decision making approach developed by T.L. Saaty where factors or criteria are arranged in a hierarchic structure (Saaty, 2000). In AHP, priorities or weights are generated by decomposing the decision making steps into the several steps: (Saaty, 2008)

1. Definition of the problem.
2. Structuring of the decision hierarchy with the goal at the top and different objectives at the lower hierarchy.
3. Constructing a set of pairwise comparison matrices. Elements in the same hierarchical level are compared to one another using a scale of numbers (Table 1).
4. Generating the weights of each element of the decision-making hierarchy based on the comparisons.

Table 1. The fundamental scale of absolute numbers (Saaty, 2008)

Intensity of Importance	Definition	Explanation
1	Equal Importance	Two activities contribute equally to the objective
2	Weak or slight	
3	Moderate Importance	Experience and judgement slightly favour one activity over another
4	Moderate plus	
5	Strong importance	Experience and judgement strongly favour one activity over another
6	Strong plus	
7	Very strong or demonstrated importance	An activity is favoured very strongly over another; its dominance demonstrated in practice
8	Very, very, strong	
9	Extreme importance	The evidence favouring one activity over another is of the highest possible order of affirmation
Reciprocals of above	If i has value x when compared to j , then j has value $1/x$ when compared to i .	A reasonable assumption
1.1 – 1.9	If the activities are very close	May be difficult to assign the best value but when compared with other contrasting activities the size of the small numbers would not be too noticeable, yet they can still indicate the relative importance of the activities.

2. OBJECTIVES, SCOPE, AND LIMITATIONS

2.1 Objectives

The objectives of the study are:

1. To assess the solar energy resource in the Central Luzon region using r.sun.
2. To validate the results of the model and determine if the appropriateness of its use in a tropical setting like the Philippines.
3. To identify possible sites for installing ground-mounted solar PV farms in the region based on different criteria.

2.2 Scope and Limitations

The study will only compute for the global component of solar radiation or the Global Horizontal Irradiation (GHI) in the Central Luzon region. The resolution of the output solar radiation maps are limited by the DEM used which is the Shuttle Radar Topography Mission (SRTM) DEM whose horizontal resolution is 90m. The computation of the real-sky radiation and its subsequent validation is also hindered by the number of solar radiation measuring stations in the region.

3. REVIEW OF RELATED LITERATURE

As a solar radiation model, r.sun is typically used in European countries or those at higher latitudes since it is based on the ESRA model (Nguyen and Pearce, 2010; Hofierka and Cebecauer, 2008; Kryza et al., 2013). It has been applied in large-scale estimation and assessment of solar radiation in Canada (Nguyen and Pearce, 2010), Slovakia (Hofierka and Cebecauer, 2008), and Poland (Kryza et al., 2013) with good and promising results in terms of accuracy.

4. METHODOLOGY

4.1 Solar Energy Resource Assessment

The datasets used in the solar energy resource assessment include a Shuttle Radar Topography Mission (SRTM) DEM (90 meter horizontal resolution) available at PhilGIS (www.philgis.com) and monthly average Linke turbidity coefficient values downloaded from the Solar Radiation Database (SoDA) webservice (www.soda-is.com). The DEM is used to compute for the slope and aspect in the region using GRASS' r.slope.aspect module. It also used to create horizon rasters using r.horizon. The Linke turbidity coefficient values are used to interpolate monthly average Linke turbidity rasters using the v.surf.rst (Regularized Spline with Tension) module.

Daily solar radiation readings from Bureau of Soils and Water Management (BSWM) sensors throughout the region were downloaded for the computation of the clear-sky index and validation of the modelled solar radiation values. To ensure the quality of the solar radiation data used, only those that met different quality control criteria in terms of the completeness of the readings were used for solving the measured monthly average GHI in the region. For each month, a minimum of eight (8) sensors with solar radiation data were available. Two (2) were chosen for validation of the modelled GHI while the remaining

sensors were used for the interpolation of the monthly clear-sky index. From the solar downloaded solar radiation data, twenty-four (24) point vector files were created (one each month for Kc interpolation and another for validation).

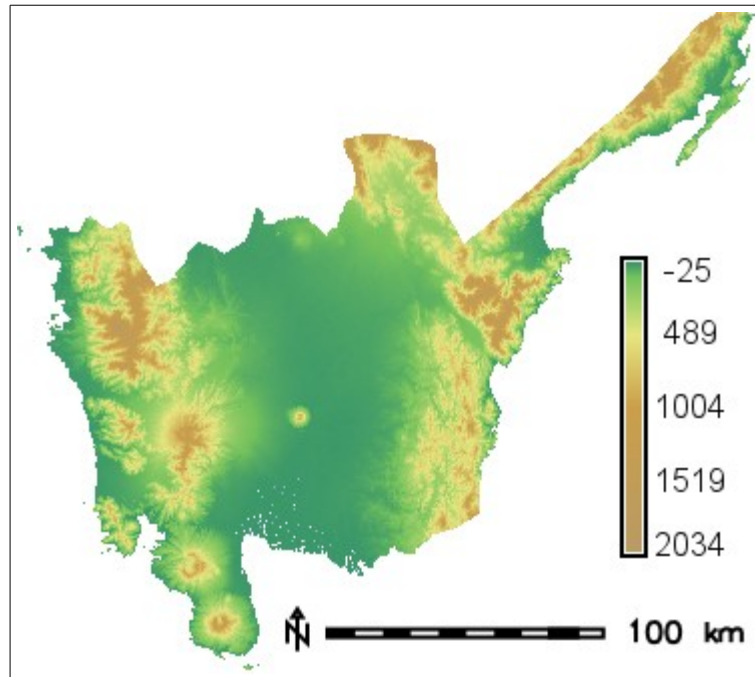


Figure 2. SRTM DEM of Region 3

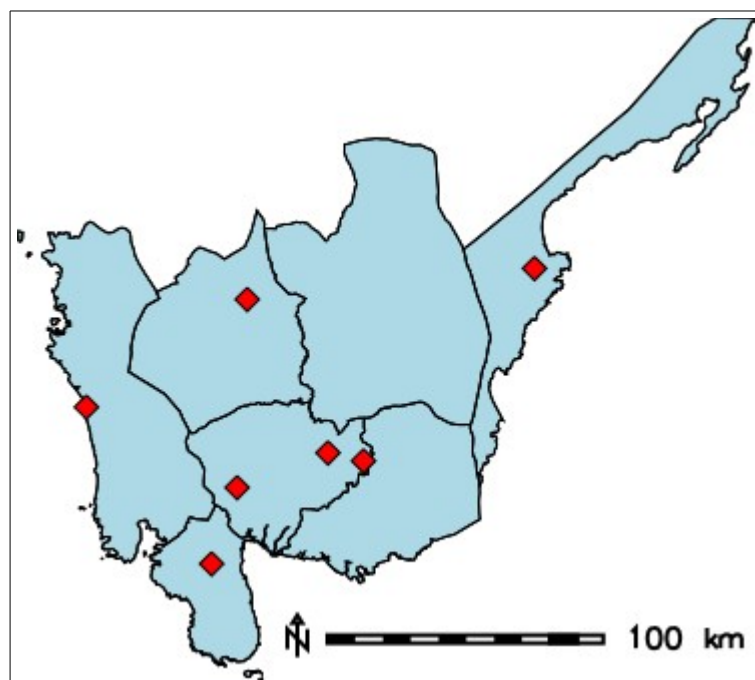


Figure 3. BSWM Solar Sensors for Kc Interpolation

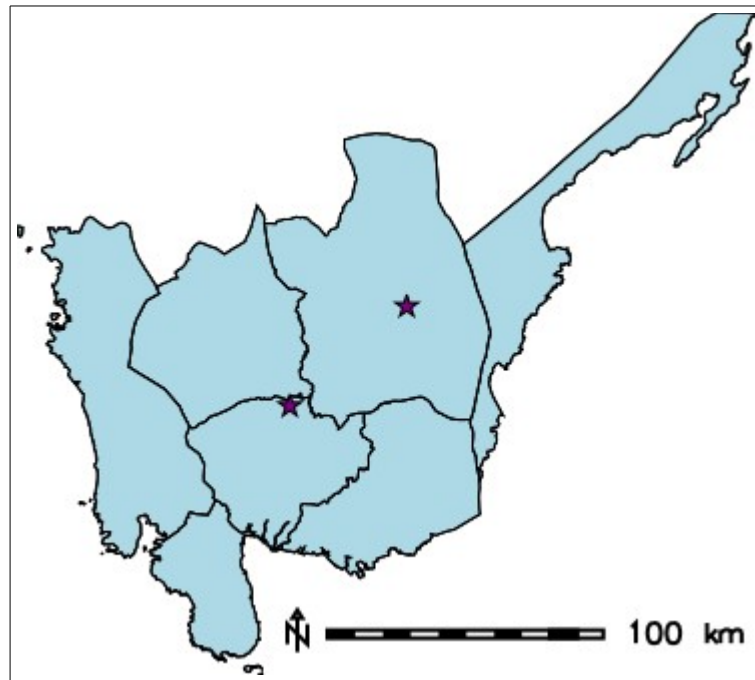


Figure 4. BSWM Solar Sensors for Validation

In order to reduce the number of model runs from 365 to 12, the Julian day and declination of the recommended average day for each month (Duffie and Beckman, 1991) was used to calculate the monthly average clear-sky GHI in the region. The values for these average days are provided below (Table 2).

Table 2. The average days for each month (Duffie and Beckman, 1991)

Month	Average Day of the Month			
	Day	Julian day	Declination (degrees)	Declination (radians)
January	17	17	-20.92	-0.3651228795
February	16	47	-12.95	-0.2260201381
March	16	75	-2.42	-0.0422369679
April	15	105	9.41	0.1642354826
May	15	135	18.79	0.3279473664
June	11	162	23.09	0.4029965243
July	17	198	21.18	0.3696607356
August	16	228	13.45	0.2347467844
September	15	258	2.22	0.0387463094
October	15	288	-9.60	-0.1675516082
November	14	318	-18.91	-0.3300417616
December	10	344	-23.05	-0.4022983926

After computation of the monthly average clear-sky GHI rasters, the clear-sky index for the BSWM sensors were calculated using equation (3). After which, monthly clear-sky index rasters were interpolated using v.surf.rst. Monthly average real-sky GHI rasters are then calculated using equation (6). The annual average real-sky GHI is computed by multiplying the monthly GHI rasters with the number of days for each month and then dividing the result by 365.

$$GHI_{real, annual} = \sum_{i=jan}^{dec} GHI_{real,i} \times \text{number of days}_i \quad (9)$$

The modelled monthly average real-sky GHI are compared with measured GHI values from the two solar radiation sensors not included in the clear-sky index interpolation in order to validate the results of r.sun. These two sensors are located in Station 916 in Pampanga and Station 929 in Nueva Ecija. For the comparison, the following statistics are computed (Zhang et al, 2013):

1. Mean Bias Error (MBE)

$$MBE = \frac{1}{n} \sum_{i=1}^n (modeled - measured) \quad (10)$$

2. Mean Absolute Error (MAE)

$$MAE = \frac{1}{n} \sum_{i=1}^n |modeled - measured| \quad (11)$$

3. Mean Absolute Percent Error (MAPE)

$$MAPE = \frac{1}{n} \sum_{i=1}^n \frac{100 \times |modeled - measured|}{measured} \quad (12)$$

4. Root-Mean Square Error (RMSE)

$$RMSE = \sqrt{\frac{\sum_{i=1}^n (modeled - measured)^2}{n}} \quad (13)$$

The workflow for the solar energy resource assessment is shown below (Figure 2).

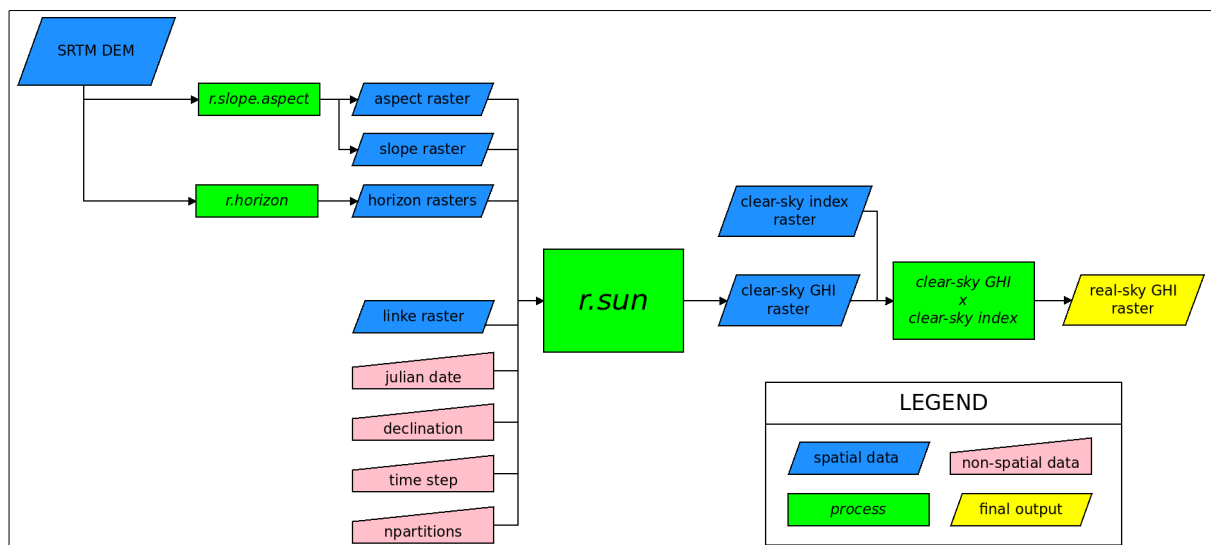


Figure 5. Solar Energy Resource Assessment Workflow

4.2 Site Suitability Analysis

Interviews with stakeholders and experts from the government, industry, environment sector, and the academe were held in order to determine the different criteria, their hierarchy, and their respective weights. From these interviews, the criteria were divided into factors and constraints. Factors are given weights and, when standardized, they have values ranging from 0 to 1. Meanwhile, constraints are used to filter the areas and have values of 0 or 1.

Table 3. Hierarchy of Criteria (Factors)

Level 0	Suitability for Ground-Mounted Solar PV Farms				
Level 1	Resource	Non-Resource			
Level 1	Annual Average GHI	Physical	Environmental	Socio-Economic	Risk
Level 2		<i>Slope</i> <i>Aspect</i> <i>Land Cover</i> <i>Proximity to water bodies</i>	<i>Protected areas</i> <i>Key biodiversity areas</i>	<i>Proximity to airports</i> <i>Proximity to grid</i> <i>Proximity to transportation networks</i> <i>Proximity to built-up areas</i>	<i>Landslide</i>

Table 4. Constraint Criteria

Constraint
<i>IP locations</i> <i>Cultural heritage sites</i> <i>Infrastructures</i> <i>Areas with high flood susceptibility</i>

The first level of the hierarchy divides the factors into resource and non-resource criteria. The non-resource criteria are then divided into four groups: Physical, Environmental, Socio-economic, and Risk.

The Physical criteria deal with the effects of the physical space on the suitability of the site including the slope and aspect of the area, its land use, and how close it is to a water source. Relatively flat areas that are south facing are preferred since these areas require less earthworks for setting up ground-mounted solar PV's. In the same vein, bare and barren areas are preferred over heavily forested ones. Lastly, the proximity to a water source is important for a steady supply of water to the solar PV plant. The Environmental criteria deal with the possible effects of the PV plant on the environment. Sites that farther away from protected and key biodiversity areas are preferred. The socio-economic criteria take into account the possible costs in putting up a ground-mounted solar PV farm in an area. Thus, sites that are closer to the grid and transportation networks are considered as better options. Lastly, the effect of landslides on the suitability of a site are considered by the Risk criteria. The standardization of the values of each criteria was done using thresholds provided by the stakeholders and literature. For the resource criteria, the stakeholders agreed on a threshold of 4000 Wh/m²-day as being suitable.

Upon determination of the criteria hierarchy, the assignment of weights for each of the criteria was performed using AHP. Eleven (11) respondents from different sectors including the policy-makers, environmentalists, academe, and industry were interviewed for the determination of criteria weights using AHP with the following results (Table 5).

Table 5. Criteria Weights using AHP

	Criteria	Weight
Level 1	Available resource	0.826
	Non-resource factors	0.174
Level 2 <i>Non-resource factors</i>	Physical	0.378
	Environmental	0.166
	Socio-economic	0.258
	Risk	0.198
Level 3 <i>Physical</i>	Slope	0.383
	Aspect	0.271
	Land Use	0.248
	Proximity to water bodies	0.098
Level 3 <i>Environmental</i>	Proximity to protected areas	0.500
	Proximity to key biodiversity areas	0.500
Level 3 <i>Socio-economic</i>	Proximity to built-up areas	0.167
	Proximity to transportation networks	0.168
	Proximity to the electricity grid	0.570
	Proximity to airports	0.095
Level 3 <i>Risk</i>	Landslide susceptibility	1.000

Weighted overlay analysis is used in order to aggregate the standardized criteria maps and produce the suitability map for ground-mounted solar PV farms in the region. The resulting site suitability map has values between 1 and 0 with 1 being the most suitable and 0 being the least suitable.

5. RESULTS AND DISCUSSION

5.1 Monthly Average and Annual Real-sky Global Horizontal Irradiation (GHI)

The measured and modelled monthly average Global Horizontal Irradiation values for Stations 916 and 929 and their comparison are shown in the figures (Figure 4, 5) and table (Table 6) below.

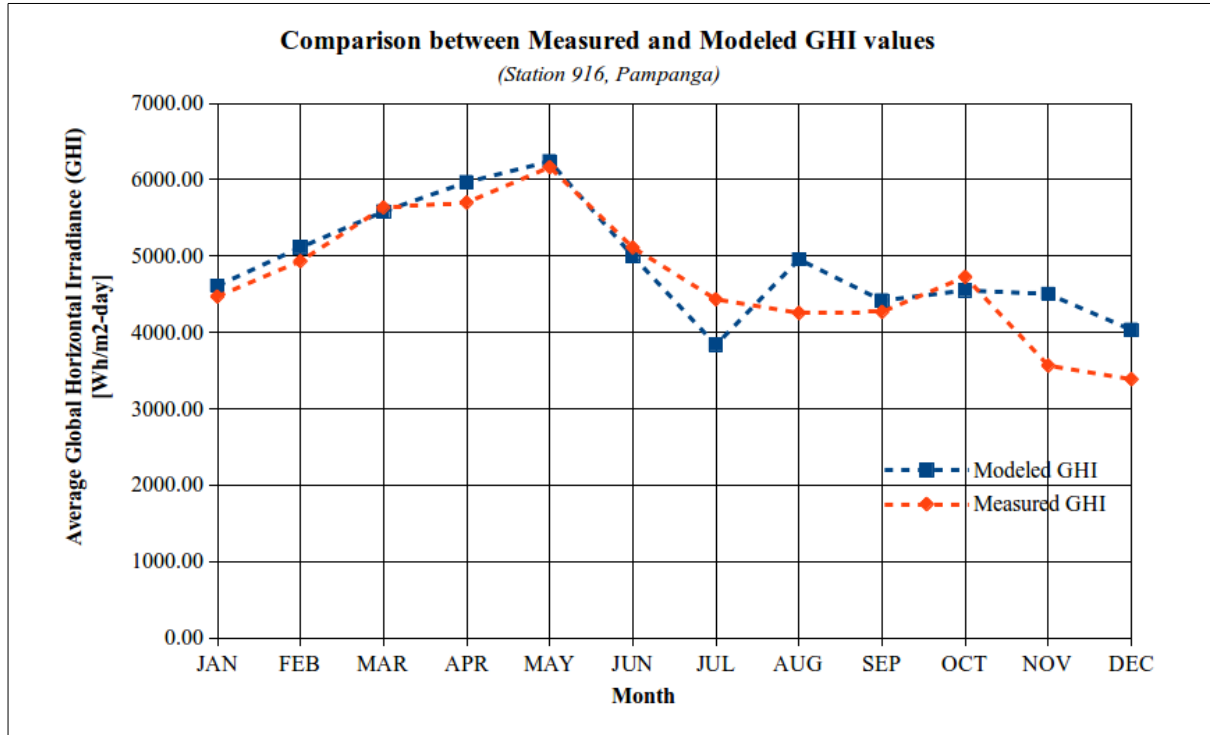


Figure 6. Measured and Modelled GHI (Station 916)

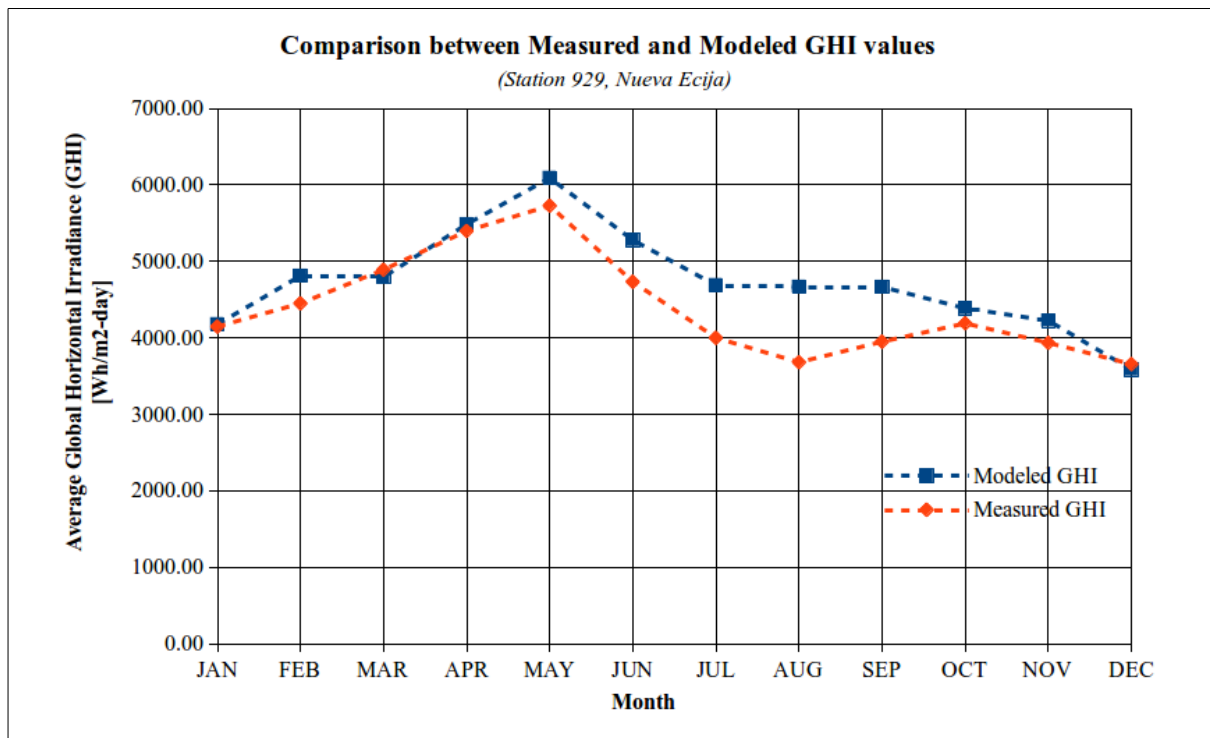


Figure 7. Measured and Modelled GHI (Station 929)

Table 6. Validation statistics of modelled GHI values

Mean Bias Error (MBE)	260.39 Wh/m ² -day
Mean Absolute Error (MAE)	352.50 Wh/m ² -day
Mean Absolute Percent Error (MAPE)	8.53%
Root-Mean Square Error (RMSE)	456.65 Wh/m ² -day

The results clearly show that the modelled GHI follow the trend of the measured GHI from the sensors with only a few large deviations (August in Sensors 916 and 929), but overall, the modelled and measured values agree with one another specially for the first half of the year. During these months, the average MAPE is only 3.84% as compared to 13.32% for the latter half of the year. The computed MBE and MAE indicate that the model typically overestimates the monthly GHI. A caveat is that only two sensors were used for validation. Using more sensors for validation is preferred, however, due to the availability of data, doing so would decrease the number used for clear-sky index interpolation. At the same time, using too few sensors for validation may lead to over-generalization of the validation results.

A summary of the modelled monthly average real-sky GHI for the region is provided below (Table 6, Figure 8).

Table 6. Monthly Average Real-sky GHI (Region 3, Philippines)

Month	Real-sky GHI (Wh/m ² -day)
JANUARY	4376.65
FEBRUARY	4929.56
MARCH	5226.91
APRIL	5672.79
MAY	6021.07
JUNE	4721.45
JULY	4301.99
AUGUST	4513.60
SEPTEMBER	4474.51
OCTOBER	4443.39
NOVEMBER	4353.56
DECEMBER	3706.80
ANNUAL	4727.12

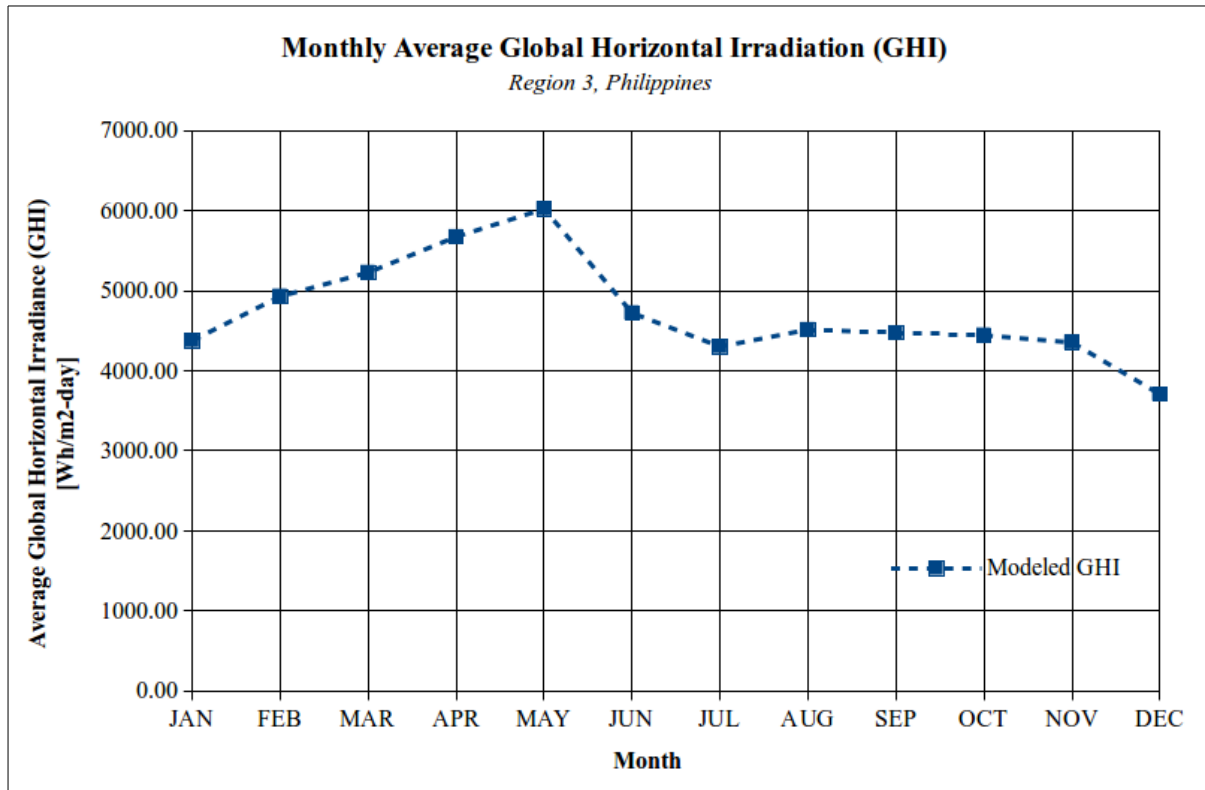


Figure 8. Monthly Average Real-sky GHI (Region 3, Philippines)

The trend in the global solar radiation received by the region is as follows: increasing from January to May, decreasing from June onwards with values from July to November being similar, and sudden drops in June and December. This trend is somewhat expected since the months from March to May are considered as summer months in the country with the hottest and clearest days coming in May. The months of July to August are considered as wet and rainy months so a decrease in the received solar radiation during these months is not surprising.

The computed annual average real-sky GHI of 4727.12 Wh/m²-day indicates a good amount of solar energy resource in the area. This is especially true from February to May whose average is 5475.16 Wh/m²-day. For the remaining months of the year, the average is 4359.60 Wh/m²-day.

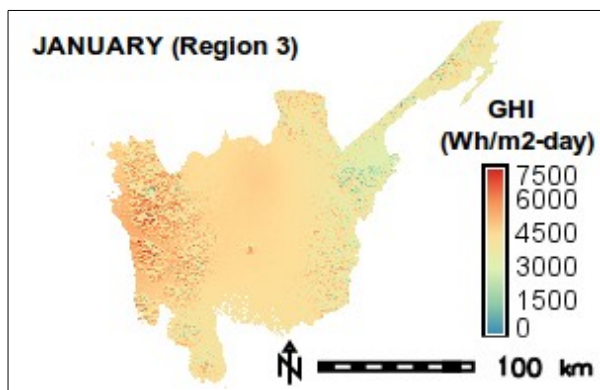


Figure 9. GHI for January

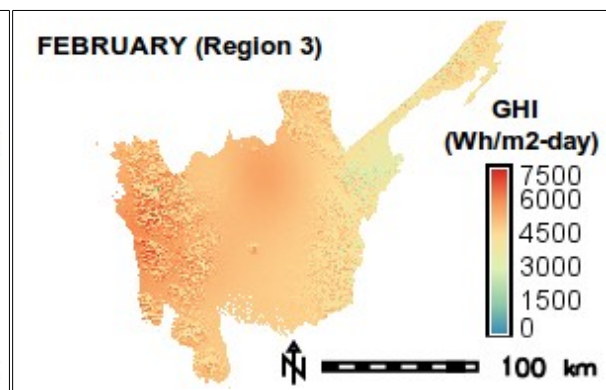


Figure 10. GHI for February

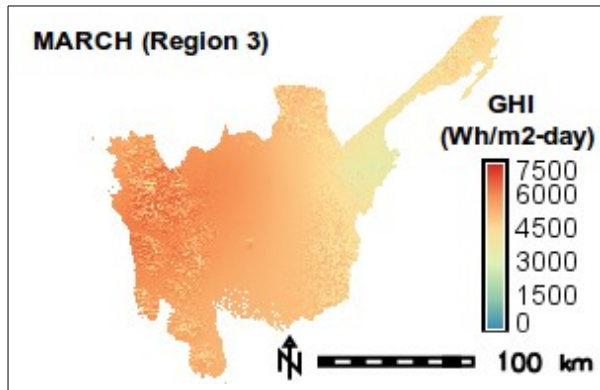


Figure 11. GHI for March

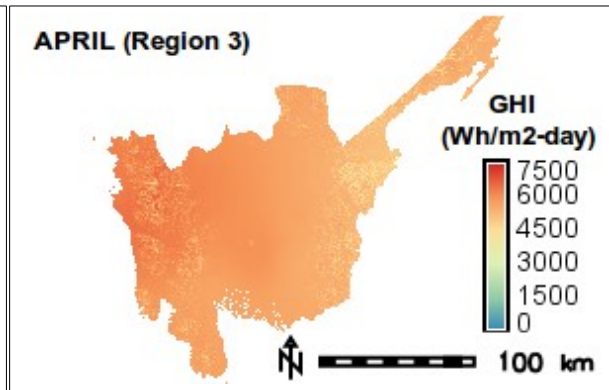


Figure 12. GHI for April

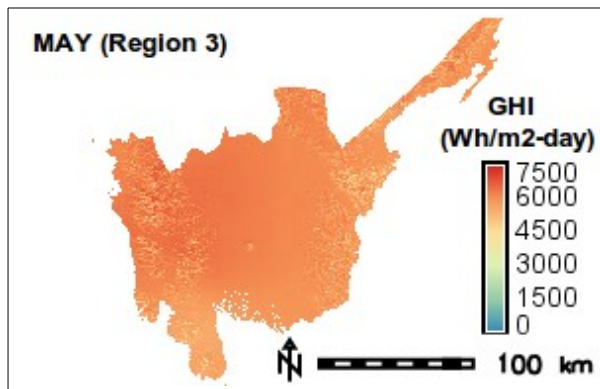


Figure 13. GHI for May

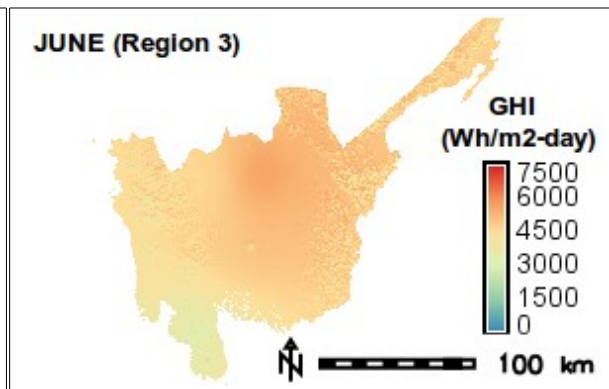


Figure 14. GHI for June

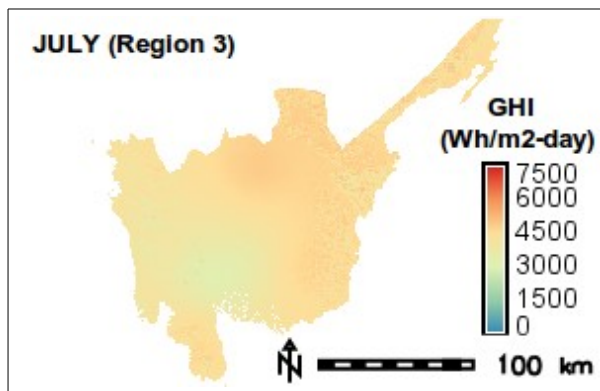


Figure 15. GHI for July

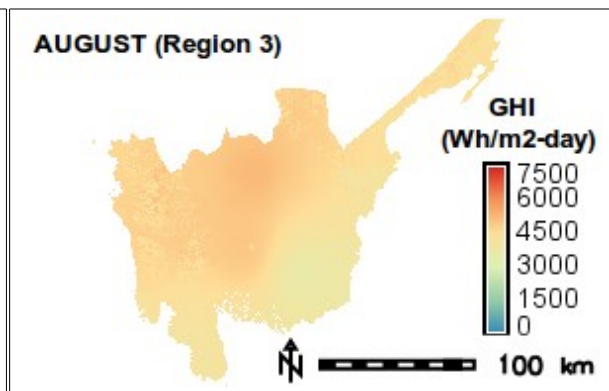


Figure 16. GHI for August

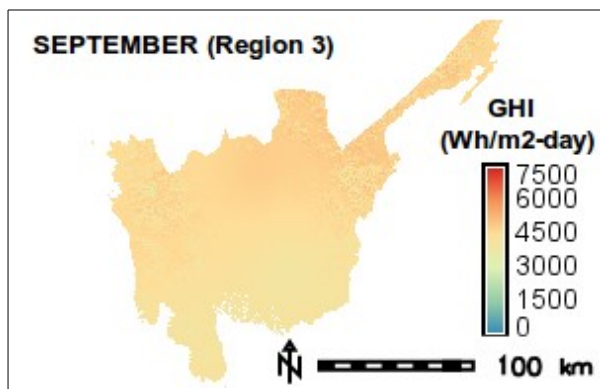


Figure 17. GHI for September

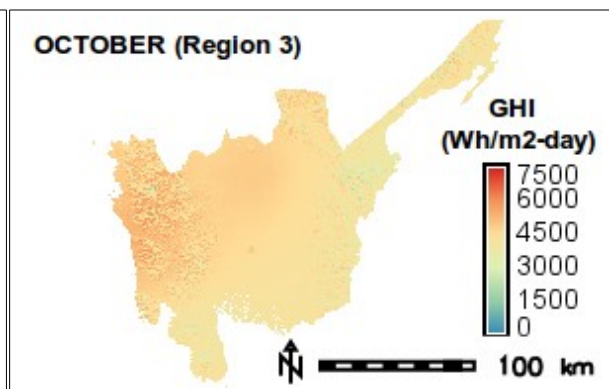


Figure 18. GHI for October

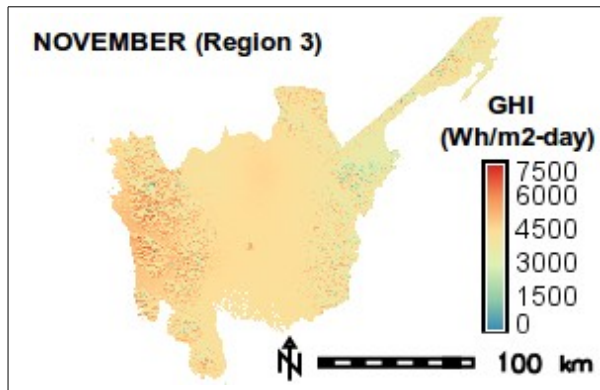


Figure 19. GHI for November

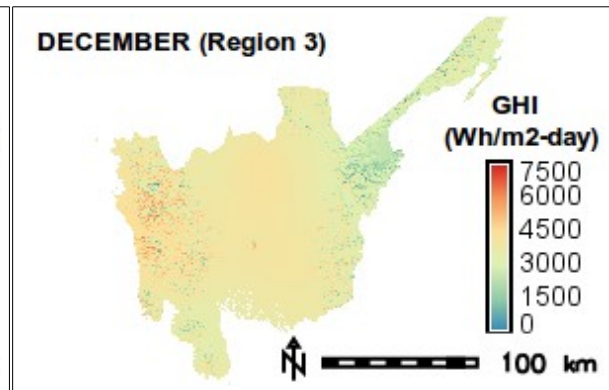


Figure 20. GHI for December

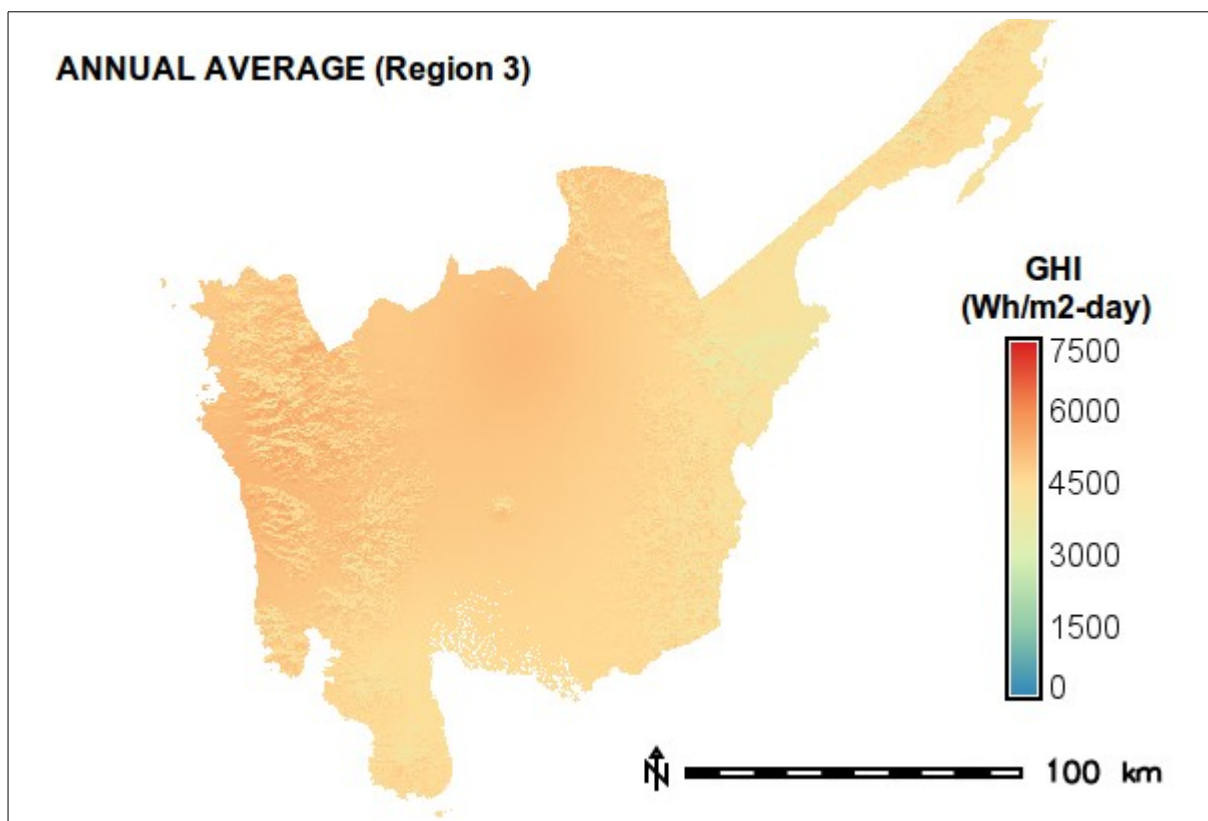


Figure 21. Annual Average GHI for Region 3

In terms of spatial variation, the western and northern parts of the region typically receive more solar radiation.

From the results, the monthly average GHI in the region computed by r.sun ranged from 3706.8 Wh/m²-day in December to 6021.0 Wh/m²-day in May with an annual average GHI of 4727.12 Wh/m²-day indicating a good amount of resource potential. High GHI values were observed for the summer months of March to May (Mean: 5640.26 Wh/m²-day) while the cold and rainy season ranging from July to December showed relatively lower values (Mean: 4298.98 Wh/m²-day). The Mean Absolute Error (MAE) and Mean Absolute Percentage Error (MAPE) between the measured and modelled GHI were 352.88 Wh/m²-day and 8.53%, respectively, with the lowest error in March (73.94 Wh/m²-day, 1.44%) and the highest in August (844.01 Wh/m²-day, 21.65%).

5.2 Suitable Sites for Ground-Mounted Solar PV Farms

The suitability maps for the resource and non-resource criteria (Physical, Environmental, Socio-economic, and Risk) are shown below.

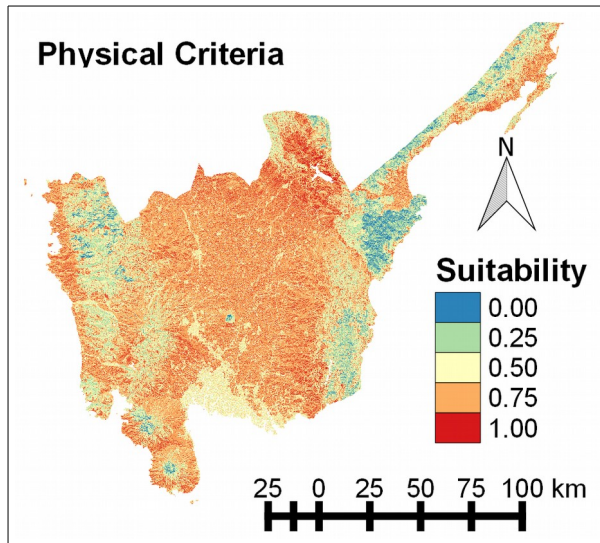


Figure 22. Physical Criteria Suitability

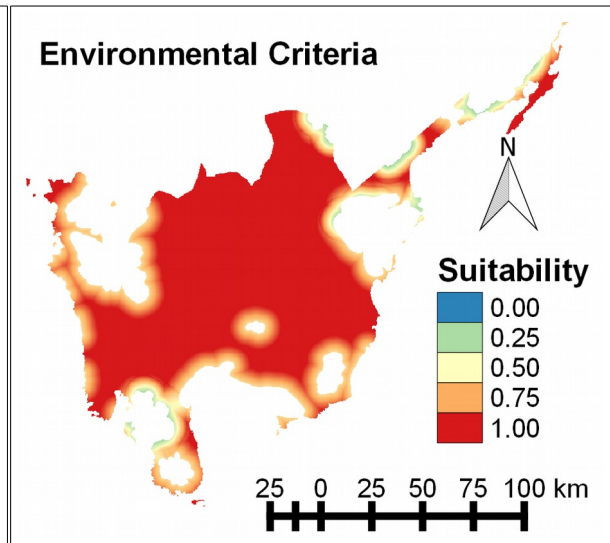


Figure 23. Environmental Criteria Suitability

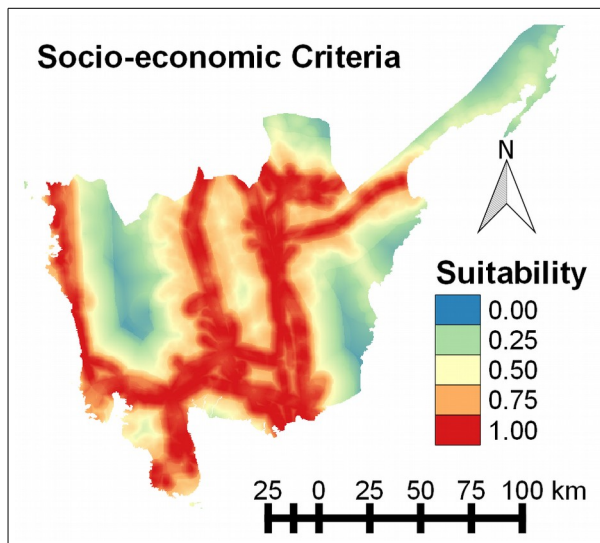


Figure 24. Socio-economic Criteria Suitability

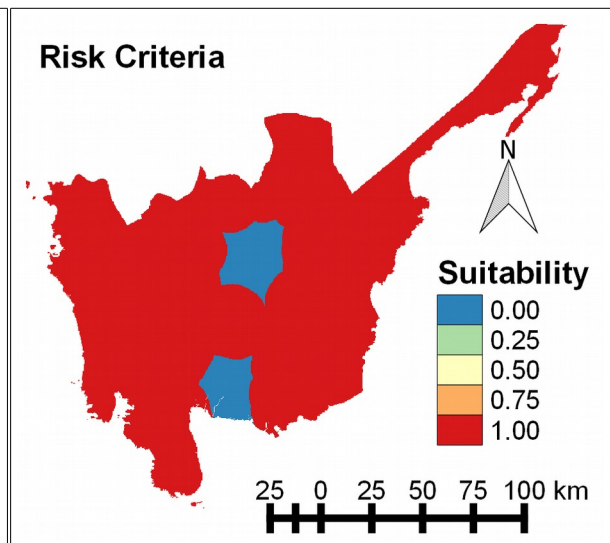


Figure 25. Risk Criteria Suitability

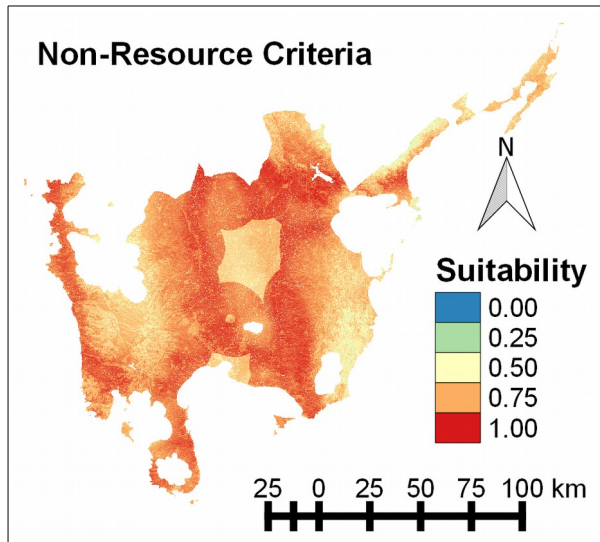


Figure 26. Non-Resource Criteria Suitability

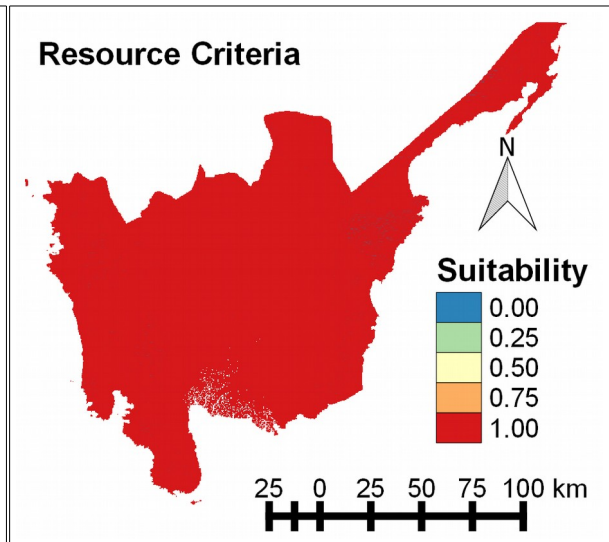


Figure 23. Resource Criteria Suitability

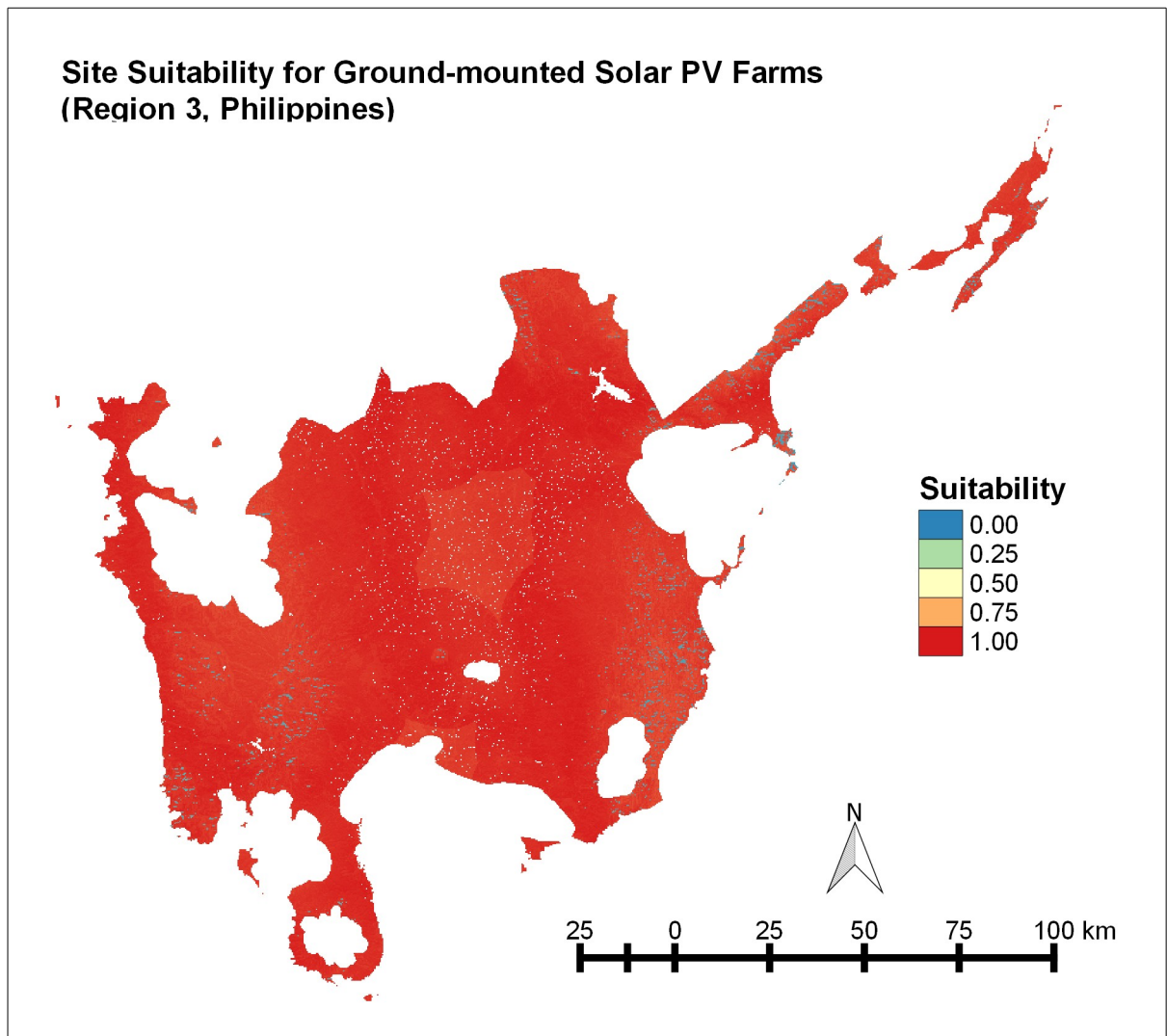


Figure 28. Site Suitability for Ground-mounted Solar PV Farms in Region 3, Philippines

Because of the high average annual GHI values in the region coupled with large weight of the resource criteria in the suitability analysis, vast portions of the region have high suitability for installing ground mounted solar PV farms.

6. CONCLUSIONS AND RECOMMENDATIONS

From the validation results, we can safely say that r.sun was able to model the incoming global solar radiation in the Central Luzon region at an acceptable, if not high, level of accuracy with a Mean Absolute Error (MAE) and Mean Absolute Percentage Error (MAPE) between the measured and modelled GHI of 352.88 Wh/m²-day and 8.53%, respectively. In fact, the model performed well for the months of January to June (MAE: 192.18 Wh/m²-day, MAPE: 3.83%) and slightly poorer for July to December (MAE: 512.824 Wh/m²-day, MAPE: 13.22%). A caveat on the validation is that only two points were used which could lead to over-generalization. For better validation results, more validation points are needed without compromising the number of points for interpolation of the clear-sky index values. One such way to do this is to compute for the Kc rasters of nearby regions and areas and use these values to interpolate the Kc rasters for the Eastern Visayas region. This would entail solving for the clear-sky GHI for those areas but would also mean that more points within the region will remain for validation of the results.

It can also be concluded that there is a good amount of solar energy resource potential in the region with with an annual daily average GHI of 4727.12 Wh/m²-day, ranging from 3706.8 Wh/m²-day in December to 6021.0 Wh/m²-day in May. This is specially true for the summer months of March to May (Mean: 5640.26 Wh/m²-day).

In terms of the site suitability, it can be seen that almost the entire region aside from the constraint areas (protected areas, flood prone, etc) is suitable for installing ground mounted solar PV farms. This can be attributed to the high GHI values in the region and the relatively large weight of the resource criteria as compared to the non-resource criteria. For better site suitability results, other datasets and criteria can be added. Fuzzy AHP can also be looked into or the weights assignment themselves can be changed.

7. REFERENCES

- GRASS Development Team, 2015. GRASS 7.0 Users Manual. Open Source Geospatial Foundation, USA. Electronic document: <http://grass.osgeo.org/grass70/manuals/>
- GRASS-Wiki. http://grasswiki.osgeo.org/wiki/Main_Page
- Duffie, J.A. and Beckman, W.A. 1991. Solar Engineering of Thermal processes, Second ed. John Wiley & Sons.
- Hofierka, J. and Cebecauer, T. 2008. "Spatially distributed assessment of solar resources for energy applications in Slovakia." *Acta Facultatis Studiorum Humanitatis et Naturae Universitatis Prešovensis. Prírodné vedy, Folia Geographica 12*, pp. 97-114.
- Hofierka, J. and Suri, M. 2002. "The solar radiation model for Open Source GIS: implementation and application". *Proceedings of the Open source GIS - GRASS users conference 2002 - Trento, Italy, 11-13 September 2002*.

- Kryza, M. et al. 2010. "Spatial information on total solar radiation: Application and evaluation of the r.sun model for the Wedel Jarlsberg Land, Svalbard." *Polish Polar Research*, vol. 31 no. 1, pp. 17-32.
- Nguyen, H.T. and Pearce, J.M. 2010. "Estimating Potential Photovoltaic Yield with r.sun and the Open Source Geographical Resources Analysis Support System." *Solar Energy* 84, pp. 831-843.
- Suri, M. and Horierka, J. 2004. "A new GIS-based solar radiation model and its application to photovoltaic assessments." *Transactions in GIS* 8 (2): pp. 175–190.
- Zhang, J. et al. 2013. "Metrics for Evaluating the Accuracy of Solar Power Forecasting." *Conference Paper: NREL/CP-5500-60142*.